



CHORUS

This is the accepted manuscript made available via CHORUS. The article has been published as:

Vanadium Dioxide: A Peierls-Mott Insulator Stable against Disorder

Cédric Weber, David D. O'Regan, Nicholas D. M. Hine, Mike C. Payne, Gabriel Kotliar, and Peter B. Littlewood

Phys. Rev. Lett. **108**, 256402 — Published 20 June 2012

DOI: [10.1103/PhysRevLett.108.256402](https://doi.org/10.1103/PhysRevLett.108.256402)

Vanadium dioxide : A Peierls-Mott insulator stable against disorder

Cédric Weber,¹ David D. O'Regan,^{1,2} Nicholas D. M. Hine,^{1,3}
Mike C. Payne,¹ Gabriel Kotliar,⁴ and Peter B. Littlewood^{1,5}

¹*Cavendish Laboratory, J. J. Thomson Av., Cambridge CB3 0HE, U.K.*

²*Theory and Simulation of Materials, École Polytechnique Fédérale de Lausanne, Station 12, 1015 Lausanne, Switzerland*

³*T.Y.C. and Materials and Physics dpt., Imperial College London, London SW7 2AZ, U.K.*

⁴*Rutgers University, 136 Frelinghuysen Road, Piscataway, NJ, U.S.A.*

⁵*Physical Sciences and Engineering, Argonne National Laboratory, Argonne, Illinois 60439, U.S.A.*

Vanadium dioxide undergoes a first order metal–insulator transition at 340 K. In this work, we develop and carry out state of the art linear scaling DFT calculations refined with non-local dynamical mean-field theory. We identify a complex mechanism, a Peierls-assisted orbital selection Mott instability, which is responsible for the insulating M_1 phase, and furthermore survives a moderate degree of disorder.

Vanadium dioxide (VO_2) undergoes a first order metal–insulator transition (MIT) at 340 K [1]. At high temperature, the crystal structure is metallic with the rutile structure (R), while it transforms to the monoclinic (M_1) phase and becomes insulating below the transition temperature. The nature of the metal-insulator transition in VO_2 has been long discussed, with particular emphasis placed on the role of electron correlations in forming the charge gap. Photoemission experiments give strong evidence for strong electron-electron and electron-phonon coupling in VO_2 [2], suggesting that this compound is an archetypal Mott insulator. However, density functional theory (DFT) predicts the M_1 phase to be metallic [3, 4]. An alternative point of view is that the low-temperature phase of VO_2 may constitute a band (Peierls) insulator, where the crystal distortion with the V-V dimerization splits the a_{1g} bonding band, as suggested early by Goodenough [5]. Lastly one should consider a charge transfer insulator exhibiting a strong mass renormalisation [6]. The purpose of this letter is to disentangle these competing pictures. The Peierls picture was supported by DFT+GW calculations, where the authors found that off-diagonal matrix elements in the self-energy opened a gap [4], although its value was almost zero and thus well below the experimental value of 0.6 eV [7]. Very recently, a model Hamiltonian approach using cluster dynamical mean-field theory (DMFT) applied to a three band Hamiltonian for the t_{2g} orbitals has been shown to successfully capture the insulating nature of the M_1 phase [8, 9], and the authors found a charge gap of 0.6 eV, in very good agreement with experiment [7]. Hence, VO_2 is, in the latter view, not a conventional Mott insulator. Instead, the formation of dynamical V-V singlet pairs due to strong Coulomb correlations is necessary to trigger the opening of a Peierls gap. We note, however, that in Ref. [8] the vanadium 3d subshell is occupied by a single electron (0.8 electrons for the a_{1g} with only 0.1 electrons remaining in each of the $e_{\pi g}$ orbitals). A general problem with model Hamiltonian approaches, recently pointed out in Ref. [10], is that the 3d

orbital density is very much affected by the orbital subset projection used in the calculations. In particular, it has been shown recently using XAS measurements [11] that the states of VO_2 are not well characterized by a single dominant ionic configuration, rather exhibiting a distributed orbital character, suggesting room for correction of Goodenough’s ionic picture of VO_2 .

The key issues that we address in this work are: (1) Is the $3d^1$ ionic picture of Goodenough valid and how many electrons are involved in the orbital selection process; (2) Can Mott correlations alone drive VO_2 to an insulator, and what is the minimal local repulsion U_d necessary to localize the charge, i.e., the Zaanen-Sawatzky-Allen (ZSA) boundary [12, 13]; (3) How is the ZSA boundary affected by other localization processes, such as the Anderson charge localization induced by disorder, and can we find an insulator for a combination of realistic disorder and Coulomb repulsion; (4) Are non-local corrections to the self energy (the Peierls mechanism) an essential ingredient to trigger the gap opening for reasonable local repulsion U_d , and is the latter insulating phase stable against external perturbations such as disorder. To address these points, we move beyond the model Hamiltonian approach and investigate the effect of correlations in a disordered prototype for the metal–insulator transition in VO_2 from the ab-initio perspective. We study the M_1 phase of VO_2 using first-principles calculations as a function of static disorder with a state of the art linear scaling DFT method [14]. The capability of linear scaling DFT to describe large super-cells, containing several hundreds of atoms, is necessary to comprehensively tackle the issue of disorder. We extend our DFT calculations with the DMFT approximation [15, 16] in order to refine the description of the strong correlations induced by the 3d subshell of the vanadium sites (for more details see the supplementary material). Throughout this work we used typical values for the screened Coulomb interaction ($U = 4$ eV) and Hund’s coupling ($J = 0.68$ eV) [17, 18], and our calculations were carried out for 324 atom super-cells (108 V atoms) and 768 atom super-cells

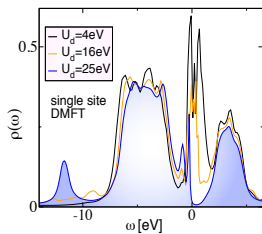


FIG. 1. (Color online) Dependence of the spectral function $\rho(\omega)$ with respect to the Coulomb repulsion U_d .

(256 V atoms) at fixed temperature $T = 189$ K. All orbitals are defined in the local coordinate system [19] associated with the vanadium atoms.

We first discuss single-site DMFT calculations for paramagnetic VO_2 . The dependence of the spectral function on the on-site repulsion U_d is shown in Fig. 1. We find that the M_1 phase of VO_2 is metallic for $U_d = 4$ eV and that there is a large spectral weight present at the Fermi level. Hence, VO_2 is described by DFT+DMFT as a charge transfer correlated paramagnetic metal, with a moderate mass renormalization $m^*/m = 1.35$, of the same order as the mass renormalization in the rutile phase obtained by other groups ($m^*/m = 1.8$ from Ref. [3] and $m^*/m = 1.51$ from Ref. [8]). The large spectral weight at the Fermi level in Fig. 1 is of predominantly d_{xy} character, the contribution from the e_g orbitals being negligible: the spin-independent orbital densities at the Fermi level $\rho_\sigma(\epsilon_F)$ are 0.02, 0.02, 0.19, 0.25, 0.28 for, respectively, $d_{x^2-y^2}, d_{3z^2-r^2}, d_{yz}, d_{xz}, d_{xy}$ symmetry, which indicates a strong selection of the t_{2g} orbitals at the Fermi level in agreement with the orbital selection scenario argued long ago by Goodenough [5]. Notably, we find that the dynamical correlations, described by the imaginary part of the self-energy, also suggest that the d_{xy} orbital is the most correlated orbital, whereas the e_g states are weakly correlated (for more details see Fig. 2 and Fig. 3 of the supplementary material). **We emphasize that here the oxygen 2p subspaces act merely as charge reservoirs, since the full Kohn-Sham Green's function is computed and then projected onto the correlated 3d subspaces. Indeed, we find that the low energy physics is obtained by the 3d orbitals near the Fermi level, in agreement with previous observation that the spectral features in VO_2 clusters are reproduced by effective Hamiltonian with 3d orbitals only [20]. However, our results deviate from the description of Goodenough: we obtain a vanadium 3d sub-shell filling of $n = 3.15$ electrons from DFT, much larger than the $3d^1$ configuration of the ionic picture. We emphasize that we used a set of local Wannier orbitals, variationally optimized during the energy minimization carried out in the DFT calculations [21], which renders the calculation of the electronic density very reliable. Larger 3d orbital occupations in VO_2 than the**

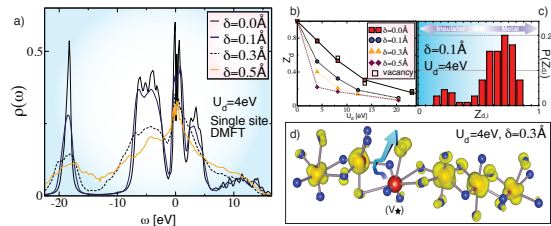


FIG. 2. (Color online) a) Spectral function ρ of paramagnetic VO_2 in the presence of Gaussian disorder δ . b) Averaged quasi-particle weight Z_d with respect to the repulsion U_d for zero ($\delta = 0$ Å) to large disorder ($\delta = 0.5$ Å). Calculations including a single O vacancy in the $\delta = 0$ Å case are also shown for comparison (open squares). c) Distribution of the local quasi-particle weight $Z_{d,i}$ for $\delta = 0.1$ Å. d) Isosurface of the real space representation of the Fermi density for disorder $\delta = 0.3$ Å. The large (small) sphere denotes V (O) atoms along the rutile axis.

single electron have been reported in earlier DFT calculations (LSDA+ U finds $n = 2.48$ e [11]). We note, furthermore, that similar occupancies are obtained for the R phase, both by experimental measurement ($n = 1.78$ e from XAS [11]) and DFT calculations (LSDA+ U finds $n = 2.31$ e [11] and LMTO-ASA gives $n = 3.35$ e [22]). For larger U_d , we find that the spectral weight at the Fermi level shrinks, and we obtain an insulator for $U_d = 25$ eV, placing VO_2 well below the ZSA boundary U_d^c , estimated between 21 eV and 25 eV. We conclude that a large 3d-3d Coulomb interaction alone is not sufficient to generate a large band gap for VO_2 , as also suggested by early LDA calculations [19, 23] which failed to reproduce the insulating state. Finally, we also explored the dependence on the Hund's coupling J and found no significant change in the mass renormalization by varying J between 0.3 eV and 1.2 eV, for fixed $U_d = 4$ eV, although increasing J enhances the mass renormalization for $U_d = 8$ eV and $U_d = 16$ eV.

If Coulomb correlations alone cannot lead to insulating behavior, perhaps the inevitable disorder due to imperfections of the crystal, or self-trapping due to strong electron-phonon coupling could be relevant. Hence we applied a random three-dimensional Gaussian displacement to both the V and O atomic sites. The Gaussian width δ characterizes the amplitude of the disorder. The spectral function for disordered VO_2 is shown in Fig. 2.a. Although the spectral weight at the Fermi level is suppressed with increasing disorder (reflecting charge localization) the system remains metallic up to the largest physical amplitudes of disorder. The effect of the localization induced by disorder is also observed in the averaged quasi-particle weight Z_d (Fig. 2.b) and in the spatial distribution of the local quasi-particle weight $Z_{d,i}$ (Fig. 2.c), which clearly shows that the disorder generates regions in the crystal with strong localization, which

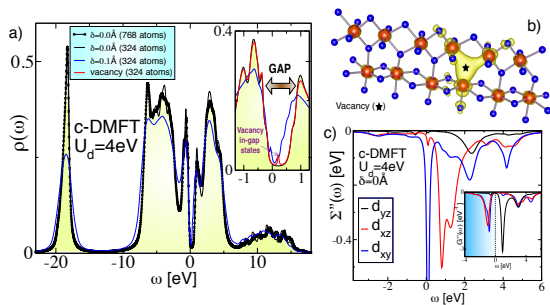


FIG. 3. (Color online) a) Spectral function ρ obtained using cellular cluster DMFT (c-DMFT) calculations without ($\delta = 0$ Å) disorder for moderate (324 atom) and large (768 atom) super-cells. Calculations for disordered VO_2 ($\delta = 0.1$ Å) and for a single O vacancy are also shown for comparison. Inset: Enlargement of the low energy scale, the gap of ~ 0.6 eV is shown. The vacancy introduces a mid-gap state, highlighted by the arrow. b) Isosurface of the real space representation of the charge density at the Fermi level for calculations for an O vacancy (star). The large (small) sphere denotes V (O) atoms along the rutile axis (horizontal direction). c) Imaginary part of the self-energy and (inset) imaginary part of the Green's function for $\delta = 0$ Å.

coexist with metallic parts of the crystal where the localization has only a weak effect. These droplets of strongly correlated Fermi liquid generate a larger mass renormalization m^*/m on average, as observed in the decrease of the averaged quasi-particle weight ($Z_d = m/m^*$) as the disorder increases (Fig. 2.b). The localization effect can be understood in a simple picture: when the O atoms move closer to the V atomic site, the static charge repulsion induces a larger charge transfer energy $\Delta = \epsilon_d - \epsilon_p$, which enhances the strength of the correlation locally (the repulsion U of the one band Hubbard model translates into the charge transfer energy in d-p theories [12]). This effect is illustrated in Fig. 2.d, where we show an isosurface of the real-space representation of the Fermi density $\rho(\epsilon_F, \tau)$ for one of the V chains along the rutile axis for $\delta = 0.3$ Å, where large (small) spheres denote V (O) atomic sites. The V atom highlighted by a star has two very near oxygen neighbors, which is expected to induce a larger charge transfer energy. The latter results in a transfer of charge from the vanadium site to one of its oxygen neighbors (indicated by an arrow). The subtle interplay between the localization induced by the disorder (Anderson-like) and the localization induced by strong correlations (Mott-like) is captured by the DFT+DMFT methodology.

We now move to the non-local cluster cellular DMFT calculations (c-DMFT). In c-DMFT, the cluster impurity of the AIM is mapped onto the $3d$ electron subspaces of a pair of V atoms forming a dimer aligned with the rutile axis. The non-locality of the self-energy between dimerized vanadium $3d$ subspaces is thereby self-consistently

included in the calculations. The non-local correlation present in cluster DMFT drives VO_2 to an insulator (Fig. 3.a), in agreement with earlier DMFT calculations using model Hamiltonians [8] and we obtain a gap of ~ 0.6 eV in agreement with both the latter and the experimental value [7]. We did not observe any finite size effect, and the Peierls gaps obtained extracted from the 324 and 768 atom super-cells are identical. We find that large disorder quenches the Peierls state for $\delta > 0.1$ Å. Very interestingly, the insulating Peierls state survives for moderate disorder $\delta = 0.1$ Å, although the gap is reduced down to ~ 0.3 eV. We also carried out cluster DMFT calculations for the case of a single O vacancy: the O vacancy creates a mid-gap state (inset of Fig. 3.a), spatially localized in the center of the three V atoms surrounding the vacancy, as illustrated by the real space representation of the Fermi level density (Fig. 3.b) but does not strongly affect the band edges. In conclusion, our results suggest that the Peierls instability in VO_2 is very robust, surviving external perturbations such as reduction of the long-range crystallographic order or local impurities. The imaginary part of the self-energy of the dynamical Peierls singlet is shown in Fig. 3.c. We observe that the gap is mainly induced by dynamical correlations in the d_{xy} orbital, which exhibit a pole at the Fermi level. In our view, the dynamical V-V dimers generate a Mott instability (the mechanism may be thus termed Peierls-Mott). In particular, the spectral weight (inset) shows that the cluster DMFT almost entirely depletes the d_{yz} orbital, leaving two electrons equally shared between the d_{xz} and d_{xy} orbitals. The lobe of the latter orbitals point towards the rutile axis, whereas the d_{yz} orbital is oriented perpendicular to this direction and thus the latter does not contribute strongly to the orbital bonding within a V-V dimer. Interestingly, therefore in our picture we find that two electrons per V atom lie in bonding orbitals, leading to a strong Mott dynamical divergence in the self-energy (Peierls-Mott). This contrasts with the picture of Ref. [8], where a single electron on each V is of bonding character and the repulsion U_d drives the bonding orbitals to a singlet configuration, following the early proposal of Sommers and Doniach [24]. In the latter picture, the repulsion energy may be dramatically reduced by the formation of the singlet state, manifested in the fact that the low-frequency behavior of the on-site component of the self-energy, that associated with the a_{1g} orbital, is linear in frequency, as opposed to a Mott insulator in which Σ'' diverges. In our picture, the non-local self-energy affects the hybridization between intra-dimer orbitals, and act to deplete the d_{yz} orbital, leaving 2 e in two orbitals per V site, in turn generating a Mott instability which creates a pole in the local self-energy (Peierls-Mott). We note that the Peierls picture in our view involves more than one electron, due to the non-trivial hybridization between the vanadium and oxygen orbitals, as recently obtained in XAS [11] and photoe-

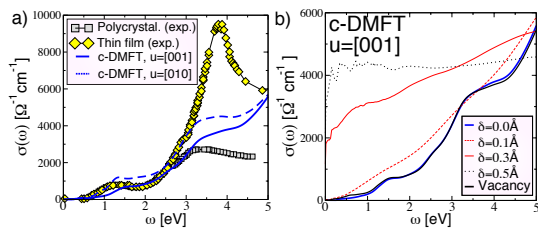


FIG. 4. (Color online) a) Theoretical optical conductivity along the rutile axis (solid lines) and along the perpendicular direction (dashed lines) calculated with cellular DMFT. Experimental data for polycrystalline films [26] (squares) and thin films (diamonds) [27] are shown for comparison. b) Optical conductivity along the rutile axis obtained by cellular DMFT for disordered VO_2 for various disorder amplitudes δ .

mission spectroscopy measurements [25], which hint at an occupation of $n \approx 2$ for the 3d sub-shell in the M_1 phase. Although we find that the low energy physics is captured by the correlated 3d orbital subspaces alone, in agreement with Ref. [20], we note that the oxygen 2p contribute indirectly to the correlations present in the 3d shell by fixing the 3d occupation, which is captured in our fully ab initio treatment. Finally, the optical conductivity calculated using cluster DMFT (Fig. 4.a) is in qualitative agreement with experimental data obtained for polycrystalline films [26] and thin films [27]. We note that the optical gap is not dramatically affected by a moderate degree of disorder $\delta = 0.1 \text{ \AA}$ (Fig. 4.b). For large disorder, however, VO_2 is a bad metal and we note, in particular, that no Drude peak is obtained in the optical conductivity, and that the disorder induces strong oscillations in the optical response for the infrared frequency range $\omega < 1 \text{ eV}$. In conclusion, we have carried out linear scaling first principle calculations, in combination with cluster DMFT, on VO_2 , both with and without disorder. We find that the ZSA boundary of the paramagnetic insulator is obtained only for unrealistic values of the Coulomb repulsion ($U_d \approx 25 \text{ eV}$). We propose a new mechanism for the insulating M_1 phase of VO_2 based on an orbital selective Mott transition, assisted by the Peierls distortion: the Peierls instability involves an orbital selection, and bonds the d_{xy} and d_{xz} orbitals along the rutile axis, filling each orbital with one electron, and in turn generates a Mott instability. This scenario may be described as *Peierls assisted orbital selective Mott transition* and reconciles the simpler one electron Peierls picture with recent soft x-ray absorption spectroscopy (XAS) [11], which points towards a breaking of the one electron per 3d orbital picture suggested early by Goodenough [5]. Finally, we demonstrated that the Peierls phase survives moderate Gaussian disorder ($\delta = 0.1 \text{ \AA}$), and hence our picture accounts for the observation of the MIT in the experimentally realistic, disordered system [28]. Finally, we found that oxygen vacancies induce

a localized mid-gap state, leaving the band edges unaffected, shedding some light on thin-film measurements where substrate strain can induce stoichiometric modification [29]. Our results, combining lattice disorder and a powerful method for describing non-local, dynamical correlation, open up new frontiers for first principles materials design under realistic experimental conditions. We are grateful to Kristjan Haule for discussions and sharing his CTQMC code. C.W. was supported by the Swiss National Foundation for Science (SNFS). D.D.O'R. was supported by EPSRC and the National University of Ireland. N.D.M.H was supported by EPSRC grant number EP/G055882/1. P.B.L is supported by the US Department of Energy under FWP 70069.

-
- [1] F. J. Morin, Phys. Rev. Lett. **3**, 34 (1959).
 - [2] K. Okazaki, H. Wadati, A. Fujimori, M. Onoda, Y. Murakawa, and Z. Hiroi, Phys. Rev. B **69**, 165104 (2004).
 - [3] A. Belozеров, A. Poteryaev, and V. Anisimov, JETP Letters **93**, 70 (2011).
 - [4] R. Sakuma, T. Miyake, and F. Aryasetiawan, Journal of Physics: Condensed Matter **21**, 064226 (2009).
 - [5] J. B. Goodenough, J. Solid State Chem. **3**, 490 (1971).
 - [6] A. E. Bocquet, T. Mizokawa, K. Morikawa, A. Fujimori, S. R. Barman, K. Maiti, D. D. Sarma, Y. Tokura, and M. Onoda, Phys. Rev. B **53**, 1161 (1996).
 - [7] T. C. Koethe, Z. Hu, M. W. Haverkort, C. Schüßler-Langeheine, F. Venturini, N. B. Brookes, O. Tjernberg, W. Reichelt, H. H. Hsieh, H.-J. Lin, C. T. Chen, and L. H. Tjeng, Phys. Rev. Lett. **97**, 116402 (2006).
 - [8] S. Biermann, A. Poteryaev, A. I. Lichtenstein, and A. Georges, Phys. Rev. Lett. **94**, 026404 (2005).
 - [9] B. Lazarovits, K. Kim, K. Haule, and G. Kotliar, Phys. Rev. B **81**, 115117 (2010).
 - [10] X. Wang, M. J. Han, L. de Medici, C. A. Marianetti, and A. J. Millis, arXiv/1110.2782.
 - [11] M. W. Haverkort, Z. Hu, A. Tanaka, W. Reichelt, S. V. Streltsov, M. A. Korotin, V. I. Anisimov, H. H. Hsieh, H.-J. Lin, C. T. Chen, D. I. Khomskii, and L. H. Tjeng, Phys. Rev. Lett. **95**, 196404 (2005).
 - [12] J. Zaanen, G. A. Sawatzky, and J. W. Allen, Phys. Rev. Lett. **55**, 418 (1985).
 - [13] W. F. Brinkman and T. M. Rice, Phys. Rev. B **2**, 4302 (1970).
 - [14] C.-K. Skylaris, P. D. Haynes, A. A. Mostofi, and M. C. Payne, Journal of Physics: Condensed Matter **17**, 5757 (2005).
 - [15] A. Georges, G. Kotliar, W. Krauth, and M. J. Rozenberg, Rev. Mod. Phys. **68**, 13 (1996).
 - [16] T. A. Maier, T. Pruschke, and M. Jarrell, Phys. Rev. B **66**, 075102 (2002).
 - [17] M. Korotin, N. Skorikov, and V. Anisimov, The Physics of Metals and Metallography **94**, 17 (2002).
 - [18] W. E. Pickett, S. C. Erwin, and E. C. Ethridge, Phys. Rev. B **58**, 1201 (1998).
 - [19] V. Eyert, Ann. Phys. (Leipzig) **11**, 650 (2002).
 - [20] A. Tanaka, Journal of the Physical Society of Japan **71**, 1091 (2002).

- [21] C.-K. Skylaris, A. A. Mostofi, P. D. Haynes, O. Diéguez, and M. C. Payne, *Phys. Rev. B* **66**, 035119 (2002).
- [22] M. Guelfucci, *Journal of Physics and Chemistry of Solids* **62**, 1961 (2001).
- [23] R. M. Wentzcovitch, W. W. Schulz, and P. B. Allen, *Phys. Rev. Lett.* **72**, 3389 (1994).
- [24] C. Sommers and S. Doniach, *Solid State Comm.* **28**, 133 (1978).
- [25] R. Zimmermann, P. Steiner, R. Claessen, F. Reinert, S. Hüfner, P. Blaha, and P. Dufek, *Journal of Physics: Condensed Matter* **11**, 1657 (1999).
- [26] M. M. Qazilbash, K. S. Burch, D. Whisler, D. Shrekenhamer, B. G. Chae, H. T. Kim, and D. N. Basov, *Phys. Rev. B* **74**, 205118 (2006).
- [27] K. Okazaki, S. Sugai, Y. Muraoka, and Z. Hiroi, *Phys. Rev. B* **73**, 165116 (2006).
- [28] F. Chudnovskii and G. Stefanovich, *Journal of Solid State Chemistry* **98**, 137 (1992).
- [29] C. Chen, Y. Zhao, X. Pan, V. Kuryatkov, A. Bernussi, M. Holtz, and Z. Fan, *Journal of Applied Physics* **110**, 023707 (2011).